Article | Received 11 April 2025; Accepted 4 July 2025; Published 28 July 2025
https://doi.org/10.55092/ae20250004

Effectiveness of harmonic balance method in analyzing superharmonic resonance frequency response of nonlinear oscillators

Guo-Peng Bai[1], Huanping Li[2,3,*], Guilin Wen[4] and Guo-Kang Er[5]

[1] State Key Laboratory of Crane Technology, Yanshan University, Qinhuangdao 066004, China

[2] School of Vehicle and Energy, Yanshan University, Qinhuangdao 066004, China

[3] Hebei Key Laboratory of Special Carrier Equipment, Yanshan University, Qinhuangdao 066004, China

[4] Hebei Innovation Center for Equipment Lightweight Design and Manufacturing, School of Mechanical Engineering, Yanshan University, Qinhuangdao 066004, China

[5] Faculty of Science and Technology, University of Macau, Macau SAR 999078, China

* Correspondence author; E-mail: lhpysu@ysu.edu.cn.

Highlights:

- Higher-order HBM reveals extra FRC peaks.
- Accuracy varies near superharmonic resonance.
- HBM effectiveness in local SHR intervals.

Abstract: This paper investigates the frequency response curve (FRC) of the nonlinear oscillator using the harmonic balance method (HBM), focusing on the accuracy of solutions in the superharmonic resonance (SHR) region. The solutions obtained with different orders of harmonic function series are verified by the numerical continuation method. It is found that for every two-order increasing in HBM, an additional peak appears in the SHR region of FRC for the system with exclusively odd-order nonlinearities, enhancing the accuracy of results. However, higher-order HBM may not always yield higher solution accuracy in some local intervals near superharmonic resonance. The advantages and disadvantages of HBM with different harmonic function series are discussed and illustrated with two examples.

Keywords: harmonic balance method; frequency response curve; nonlinear oscillator; superharmonic resonance

1. Introduction

The analysis of nonlinear oscillators subjected to deterministic excitation is inherently challenging due to the absence of exact solutions. In the past one hundred years, researchers never stop searching for the

Copyright©2025 by the authors. Published by ELSP. This work is licensed under a Creative Commons Attribution 4.0 International License, which permits unrestricted use, distribution, and reproduction in any medium provided the original work is properly cited.

approximate solutions of nonlinear oscillators. As part of these studies, researchers developed semi-analytical and numerical methods to analyze the dynamics of physical systems governed by Duffing [1] and other nonlinear oscillators [2–5]. Semi-analytical methods mainly includes harmonic balanced method (HBM) [6], equivalent linearization method (ELM) [4] , energy balance method [7], homotopy analysis method [8] , perturbation or improved perturbation method [9]. The numerical method includes Euler's method [10], Runge-Kutta method [11,12] and numerical continuation method (NCM) [13,14]. HBM approximates the solution of a nonlinear oscillator as a series of harmonic components. By balancing the coefficients of these harmonics, the unknown parameters in the solution can be determined numerically [15]. Since an infinite harmonic series is computationally impractical, a truncated series meeting accuracy requirements is usually adopted, significantly reducing computational effort. HBM was widely employed to get the approximate solutions of nonlinear oscillators. In 1968, Baily established that higher-order harmonic amplitudes exhibit rapid frequency-domain decay, enabling finite-term approximations despite the series' infinite nature [6]. In 1976, Nakhla and Vlach developed a piecewise HBM to provide enhanced capability in capturing nonlinear periodic responses [16]. In 2009, Lai and others combined Newton's method with HBM to obtain the accurate approximate analytical higher-order solutions of strongly nonlinear Duffing oscillators with cubic-quintic nonlinear restoring force [17]. In 2010, Liu and Kalmár-Nagy demonstrated the utility of the high-dimensional harmonic balance for locating limit cycles of second-order delay-differential [18]. In 2014, Luongo and Zulli proposed a mixed multiple scale HBM to solve a general class of nonlinear multi-degree-of-freedom mechanical systems subjected to aeroelastic forces and nearby Hopf bifurcation [19]. In 2016, Hosen applied HBM to determine the approximate analytical solutions of strongly nonlinear Duffing oscillators with cubic-quintic nonlinear restoring force [20]. In 2018, Niu and others explored an improved incremental HBM which can simplify the calculation process for the strongly nonlinear systems with high-order nonlinear terms [21]. In 2022, Taghipour applied the HBM to a Duffing oscillator with a harmonic excitation [22]. It can be seen that HBM is an efficient tool for both steady-state analysis of nonlinear oscillators and frequency response curve (FRC) characterization. Among the other methods mentioned above, ELM shares a theoretical connection with HBM. It was found that ELM is equivalent to the 1st-order HBM [23]. Since HBM can be extended to higher-order approximations, it offers a broader range of applicability.

In nonlinear vibration systems, predominant research efforts have focused on high-amplitude responses near primary resonances, while amplitude characteristics at secondary resonances remain insufficiently characterized. For primary resonance analysis, both ELM and 1st-order HBM can accurately capture large response amplitudes. However, for secondary resonances, ELM becomes inadequate, necessitating the application of higher-order HBM. These secondary resonance analyses often present considerable computational challenges. In 1979, Nayfeh summarized the concept of superharmonic resonance and provided some methods to deal with superharmonic resonance in single-degree-of-freedom system under the influence of monofrequency excitation [2]. In 2005, Kim compared the experimental results with HBM simulation results, then applied multi-term HBM for a torsional nonlinear sub-system and presented analytical predictions for both super and sub-harmonic resonances [15]. In 2016, Yang investigated the response to the low-frequency of a bistable system perturbed by a low-frequency and a high-frequency excitation and found the vibrational subharmonic resonance and vibrational superharmonic resonance [24]. In 2019,

Uspensky and others proposed a method by combining Shaw-Pierre nonlinear modes and the Rauscher's approach to determine the super-harmonic resonance for strongly nonlinear piecewise linear systems [25]. Also in 2019, Li and others investigated the superharmonic resonance (SR) of the size-dependent cantilever microbeams both experimentally and analytically [26]. In 2021, Zhang examined the 1/3 subharmonic resonance and the 3rd superharmonic resonance of simply-supported shape memory alloy laminated beams [27]. While HBM has been widely applied to nonlinear systems, its effectiveness in capturing superharmonic resonance phenomena has received limited attention. The present work systematically examines HBM's performance in analyzing the frequency response curve (FRC) of nonlinear oscillators in the superharmonic resonance (SHR) region. This study is organized into three main components: (1) formulation of algebraic equations for parameter determination using 1st-, 3rd-, and 5th-order HBM; (2) development of a numerical solution procedure for solving the nonlinear algebraic equations; and (3) comprehensive evaluation through two representative nonlinear systems—the classical Duffing oscillator and an oscillator with cubic nonlinearities in both displacement and velocity. The HBM solutions are rigorously compared with numerical continuation method (NCM) benchmarks, including detailed error analysis. Numerical experiments on these strongly nonlinear systems with large nonlinear coefficients demonstrate HBM's effectiveness in characterizing superharmonic resonance frequency responses.

2. Harmonic balanced method: 1st-, 3rd-, and 5th-order algebraic equations

In the analysis of system dynamics, the steady-state response is an important component. HBM assumes that the steady-state response can be expressed as a combination of sinusoids, which exhibit periodic characteristics in the time domain. By balancing the sinusoids in the oscillator, algebraic equations can be formulated based on the coefficients of harmonics in the approximate solution expression. The accuracy of the solution depends on the number or order of harmonic terms included in the approximate solution expression. In the following text, the nonlinear algebraic equations of 1st-, 3rd-, and 5th order are given, respectively, for determining the unknown parameters in the solution expression. A damped Duffing oscillator is considered to demonstrate the solution procedures for different harmonic orders [12,20]:

$$\ddot{y} + 2\xi\omega_0\dot{y} + \omega_0^2 y + \varepsilon y^3 = A\sin\omega t \tag{1}$$

where y, $\dot{y}$ and $\ddot{y}$ denote the displacement, velocity and acceleration of oscillator, respectively; ω_0 denotes the natural frequency; ξ is the damping ratio; ε is the coefficient of nonlinear term; ω is the frequency variable of external excitation; and A is the amplitude.

The solution of Nth-order HBM can be expressed as [6,15]

$$y = a_0 + \sum_{j=1}^{N}(a_j\cos j\omega t + b_j\sin j\omega t) \tag{2}$$

2.1. 1st-order solution

In Equation (2), $N = 1$ corresponds to the 1st-order HBM. Since there is no quadratic term in Equation (1), all even-order terms in Equation (2) can be zeros, which means that $a_k = 0$, $b_k = 0$ (k is positive even number), and $a_0 = 0$. Equation (2) can be simplified as $y = a_1\cos\omega t + b_1\sin\omega t$, which given $\dot{y} = -\omega a_1\sin\omega t + \omega b_1\cos\omega t$ and $\ddot{y} = -\omega^2 a_1\cos\omega t - \omega^2 b_1\sin\omega t$. Substituting the expressions of y, $\dot{y}$ and $\ddot{y}$ into Equation (1), 1st-order algebraic Equations can be formulated as

$$\begin{cases} \frac{3}{4}\varepsilon a_1(a_1^2+b_1^2)+a_1(\omega_0^2-\omega^2)+2\xi\omega_0\omega b_1=0 \\ \frac{3}{4}\varepsilon b_1(a_1^2+b_1^2)+b_1(\omega_0^2-\omega^2)-2\xi\omega_0\omega a_1-A=0 \end{cases} \tag{3}$$

When the values of system parameters (ξ, ω_0, A, ε and ω) are given, a_1 and b_1 can be determined by solving Equations (3) numerically. By substituting different values of ω, the relation between the response amplitude y_A and excitation frequency can be discovered. For 1st-order algebraic equations, this relation can be obtained analytically. The 1st-order HBM gives

$$y_A=\sqrt{a_1^2+b_1^2} \tag{4}$$

Substituting Equation (4) into Equation (3), one has

$$\begin{cases} \frac{a_1}{2\xi\omega_0}\left(\frac{3\varepsilon}{4}y_A^2+\omega_0^2-\omega^2\right)=-\omega b_1 & (5) \\ \frac{b_1}{2\xi\omega_0}\left(\frac{3\varepsilon}{4}y_A^2+\omega_0^2-\omega^2\right)=\frac{A}{2\xi\omega_0}+\omega a_1 & (6) \end{cases}$$

Dividing Equation (6) by Equation (5) gives $\frac{b_1}{a_1}=\frac{A/(2\xi\omega_0)+\omega a_1}{-\omega b_1}$.

Further, one has

$$a_1=-\frac{2\xi\omega_0\omega y_A^2}{A} \tag{7}$$

$$b_1=\frac{y_A^2}{A}\left(\frac{3\varepsilon}{4}y_A^2+\omega_0^2-\omega^2\right) \tag{8}$$

Thus, the relationship between response amplitude and excitation frequency can be explicitly expressed as

$$\left(\frac{2\xi\omega_0}{A}\right)^2\omega^2y_A^2+\left(\frac{3\varepsilon}{4}y_A^2+\omega_0^2-\omega^2\right)^2\frac{y_A^2}{A^2}-1=0 \tag{9}$$

2.2. 3rd-order solution

The solution of 3rd-order HBM can be expressed as

$$y=a_1\cos\omega t+b_1\sin\omega t+a_3\cos 3\omega t+b_3\sin 3\omega t \tag{10}$$

With the expressions of y, $\dot{y}$ and $\ddot{y}$, the 3rd-order algebraic equations can be formulated as

$$\begin{cases} \varepsilon\left[\frac{3a_1}{4}(a_1^2+b_1^2)+\frac{3a_1}{2}(a_3^2-b_1b_3+b_3^2)+\frac{3a_3}{4}(a_1^2-b_1^2)\right]+(\omega_0^2-\omega^2)a_1+2\xi\omega_0\omega b_1=0 \\ \varepsilon\left[\frac{a_1}{4}(a_1^2-3b_1^2)+\frac{3a_3}{2}(a_1^2+b_1^2)+\frac{3a_3}{4}(a_3^2+b_3^2)\right]+(\omega_0^2-9\omega^2)a_3+6\xi\omega_0\omega b_3=0 \\ \varepsilon\left[\frac{3b_1}{4}(a_1^2+b_1^2)+\frac{3b_1}{2}(a_3^2-a_1a_3+b_3^2)+\frac{3b_3}{4}(a_1^2-b_1^2)\right]+(\omega_0^2-\omega^2)b_1-2\xi\omega_0\omega a_1-A=0 \\ \varepsilon\left[-\frac{b_1}{4}(b_1^2-3a_1^2)+\frac{3b_3}{2}(a_1^2+b_1^2)+\frac{3b_3}{4}(a_3^2+b_3^2)\right]+(\omega_0^2-9\omega^2)b_3-6\xi\omega_0\omega a_3=0 \end{cases} \tag{11}$$

Equation (11) consists of four algebraic equations that implicitly express the relationship between the response amplitude y_A and the excitation frequency ω. The unknown solution parameters a_1, b_1, a_3 and b_3 can be determined numerically when system parameters ξ, ω_0, A, ε and ω are given. Thus, the relationship between y_A and ω can be discovered numerically.

2.3. 5th-order solution

The solution form of 5th-order HBM can be expressed as

$$y = a_1 \cos \omega t + b_1 \sin \omega t + a_3 \cos 3\omega t + b_3 \sin 3\omega t + a_5 \cos 5\omega t + b_5 \sin 5\omega t \tag{12}$$

As the harmonic order increases, both the number and complexity of the algebraic equations increase. The HBM implemented in this study considers nonlinear system responses up to the fifth harmonic order. Higher-order algebraic equations are suggested to be derived using symbolic calculation through a program and not included here. The fifth-order HBM yields six nonlinear algebraic equations, expressed in terms of six unknowns a_1, b_1, a_3, b_3, a_5 and b_5, as shown in Equation (13). There are six algebraic equations in Equation (13) that implicitly express the relationship between y_A and ω. The unknown solution parameters can be determined numerically for specified values of ξ, ω_0, A, ε and ω.

The nonlinear algebraic equations can be solved numerically via the Newton-Raphson method, enabling the generation of FRCs for various harmonic orders.

$$\begin{cases}
\varepsilon\left[\frac{3a_1}{4}(a_1^2+b_1^2)+\frac{3a_3}{4}(a_1^2-b_1^2)+\frac{3a_1}{2}(a_3^2-b_1b_3+b_3^2)\right]+\varepsilon\left[\frac{3a_1}{2}(a_5^2+b_5^2)+\frac{3a_5}{4}(a_3^2-b_3^2)\right. \\
\left.+\frac{3a_5}{2}(a_1a_3+b_1b_3)-\frac{3b_5}{2}(a_1b_3+a_3b_3+a_3b_1)\right]+(\omega_0^2-\omega^2)a_1+2\xi\omega_0\omega b_1=0 \\
\varepsilon\left[\frac{a_1}{4}(a_1^2-3b_1^2)+\frac{3a_3}{2}(a_1^2+b_1^2)+\frac{3a_3}{4}(a_3^2+b_3^2)\right]+\varepsilon\left[\frac{3a_3}{2}(a_5^2+b_5^2)+\frac{3a_5}{4}(a_1^2-b_1^2)\right. \\
\left.+\frac{3a_5}{2}(a_1a_3-b_1b_3)-\frac{3b_5}{2}(a_1b_1+a_1b_3-a_3b_1)\right]+(\omega_0^2-9\omega^2)a_3+6\xi\omega_0\omega b_3=0 \\
\varepsilon\left[\frac{3a_3}{4}(a_1^2+b_1^2)+\frac{3a_1}{4}(a_3^2-b_3^2)+\frac{3b_1b_3}{2}(a_1+a_3)\right]+\varepsilon\left[\frac{3a_5}{2}(a_1^2+b_1^2)+\frac{3a_5}{2}(a_3^2+b_3^2)\right. \\
\left.+\frac{3a_5}{4}(a_5^2+b_5^2)\right]+(\omega_0^2-25\omega^2)a_5+10\xi\omega_0\omega b_5=0 \\
\varepsilon\left[\frac{3b_1}{4}(a_1^2+b_1^2)+\frac{3b_3}{4}(a_1^2-b_1^2)+\frac{3b_1}{2}(a_3^2-a_1a_3+b_3^2)\right]+\varepsilon\left[\frac{3b_1}{2}(a_5^2+b_5^2)+\frac{3b_5}{4}(-a_3^2+b_3^2)\right. \\
\left.+\frac{3b_5}{2}(a_1a_3+b_1b_3)-\frac{3a_5}{2}(a_1b_3-a_3b_3-a_3b_1)\right]+(\omega_0^2-\omega^2)b_1-2\xi\omega_0\omega a_1-A=0 \\
\varepsilon\left[-\frac{b_1}{4}(b_1^2-3a_1^2)+\frac{3b_3}{2}(a_1^2+b_1^2)+\frac{3b_3}{4}(a_3^2+b_3^2)\right]+\varepsilon\left[\frac{3b_3}{2}(a_5^2+b_5^2)+\frac{3b_5}{4}(a_1^2-b_1^2)\right. \\
\left.+\frac{3b_5}{2}(a_1a_3-b_1b_3)-\frac{3a_5}{2}(a_1b_1+a_1b_3-a_3b_1)\right]+(\omega_0^2-9\omega^2)b_3-6\xi\omega_0\omega a_3=0 \\
\varepsilon\left[\frac{3b_3}{4}(a_1^2-b_1^2)+\frac{3b_1}{4}(-a_3^2+b_3^2)+\frac{3a_1a_3}{2}(b_1+b_3)\right]+\varepsilon\left[\frac{3b_5}{2}(a_1^2+b_1^2)+\frac{3b_5}{2}(a_3^2+b_3^2)\right. \\
\left.+\frac{3b_5}{4}(a_5^2+b_5^2)\right]+(\omega_0^2-25\omega^2)b_5+10\xi\omega_0\omega a_5=0
\end{cases} \tag{13}$$

3. Numerical solution procedure

The nonlinear algebraic equations derived above can be expressed in general form as

$$f_j(a_1,b_1,a_3,b_3,\cdots,a_N,b_N)=0 \quad (j=1,2,\cdots,n) \tag{14}$$

where f_j $(j = 1, 2, \cdots, n)$ denotes the jth equation in Equations (11) or (13). The integer n counts both the number of algebraic equations and unknown solution parameters. N denotes the order of HBM, which determines the system size through the relation $n = N + 1$. This scaling holds for all harmonic balance solutions developed herein. Setting $\boldsymbol{x}_i = \{a_{1,i}, b_{1,i}, a_{3,i}, b_{3,i}, \cdots, a_{N,i}, b_{N,i}\}^T$ which is the value of $\boldsymbol{x}$ at ith iteration. The Newton-Raphson method [28] can be applied to get $\boldsymbol{x}_{i+1}$ as

$$\boldsymbol{x}_{i+1} = \boldsymbol{x}_i - \boldsymbol{F}'(\boldsymbol{x}_i)^{-1}\boldsymbol{F}(\boldsymbol{x}_i)$$

where $\boldsymbol{F}$ and Jacobian matrix $\boldsymbol{F}'$ are given as

$$\boldsymbol{F} = \begin{bmatrix} f_1 \\ f_2 \\ \vdots \\ f_n \end{bmatrix}_{n\times 1} \qquad \boldsymbol{F}' = \begin{bmatrix} \frac{\partial f_1}{\partial a_1} & \cdots & \frac{\partial f_1}{\partial b_N} \\ \vdots & \ddots & \vdots \\ \frac{\partial f_n}{\partial a_1} & \cdots & \frac{\partial f_n}{\partial b_N} \end{bmatrix}_{n\times n}$$

Numerical solution procedure requires the initial values $\boldsymbol{x}_0 = \{a_{1,0}, b_{1,0}, a_{3,0}, b_{3,0}, \cdots\}^T$, which can be got from lower order solution. For instance, the 3rd- or 5th-order HBM can use the 1st-order analytic solution $a_{1,0}$ and $b_{1,0}$ as initials (other unknowns can be set as zero). In addition, initializing the solver with results from adjacent harmonic orders is able to enhance solution precision and accelerate convergence in the numerical procedure. The iterative process terminates when the Euclidean norm of the residual vector satisfies the convergence criterion

$$\|\boldsymbol{x}_{i+1} - \boldsymbol{x}_i\|_2 < e_m$$

where e_m is the allowable error, and

$$\|\boldsymbol{x}_{i+1} - \boldsymbol{x}_i\|_2 = \sqrt{(a_{1,i+1} - a_{1,i})^2 + \cdots + (b_{N,i+1} - b_{N,i})^2}$$

For a solution of given order, the vector $\boldsymbol{x}$ corresponding to a specific excitation frequency can be computed. This solution then serves as the initial guess for the subsequent frequency step in the continuation procedure, with a sufficiently small frequency increment to ensure convergence.

4. Numerical examples

4.1. Example 1: damped duffing oscillator

The parameter values in Equation (1) are given as $\xi = 0.1$, $\omega_0 = 1$, $A = 1$ and $\varepsilon = 1$. In this case, the oscillator nonlinearity is strongly hardening and the oscillator equation is

$$\ddot{y} + 0.2\dot{y} + y + y^3 = \sin \omega t \tag{15}$$

1st-order HBM yields an explicit frequency-amplitude relationship via Equation (9),

$$\frac{\omega^2 y_A^2}{25} + y_A^2\left(\frac{3}{4}y_A^2 - \omega^2 + 1\right)^2 - 1 = 0 \tag{16}$$

The FRC of 1st-order HBM can be obtained by Equation (16). The results are validated against reference solutions computed via NCM, which is implemented using the Matcont program [14,29]. The FRCs obtained by the 1st-order HBM and NCM are shown and compared in Figure 1.

NCM generates a FRC characterized by five key points:

(1) Point A: left endpoint of the FRC;

(2) Point B: local maximum amplitude in the SHR region;

(3) Point *C*: primary resonance peak;

(4) Point *D*: stability boundary (lower amplitude limit);

(5) Point *E*: an arbitrary point on the lower stable branch.

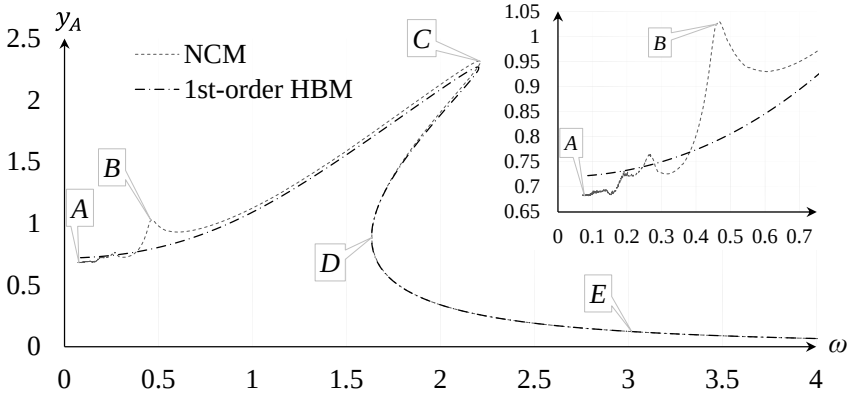


Figure 1. FRCs obtained by the 1st-order HBM and NCM.

Figure 1 reveals close agreement between 1st-order HBM predictions and NCM benchmarks in the *D*–*E* portion of the FRC, validating the solution accuracy in the high-frequency domain. However, the 1st-order HBM solution shows notable inaccuracies in the *A*–*C* segment (Figure 1), particularly at the superharmonic resonance peak (Point *B*), where amplitudes diverge by up to 23% from NCM benchmarks. This limitation, visually emphasized in the upper-right inset's magnified SHR region, underscores the need for higher-order HBM approximations when analyzing strong nonlinear systems near superharmonic resonance.

When 3rd-order HBM is applied, the solution accuracy of *A*–*C* segment shows marked improvement relative to the 1st-order one. Comparative results in Figure 2 indicate that discrepancies with NCM references are reduced from 23% to 5% at the superharmonic peak (Point *B*). However, at the intermediate second peak of segment *A*–*B*, the third-order HBM solution shows progressively increasing errors: from 3% (1st-order) to 11% (3rd-order), suggesting that the current order approximation remains insufficient for complete characterization of this nonlinear system. In order to further improve the result given by HBM, the 5th-order solution is adopted. The 5th-order solution and NCM are shown and compared in Figure 3.

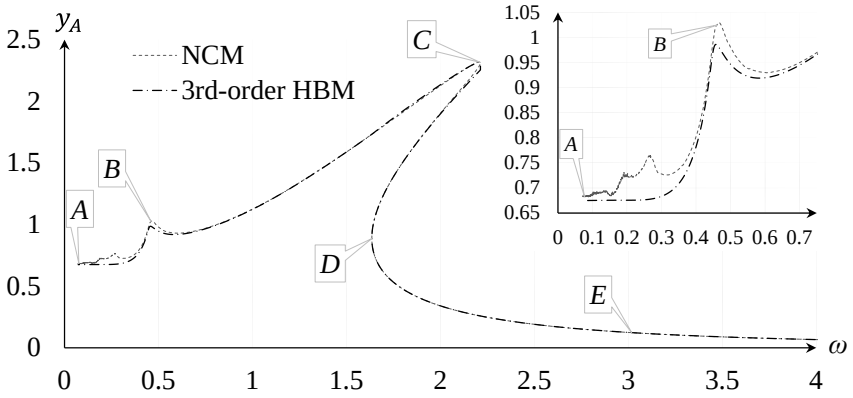


Figure 2. FRCs obtained by the 3rd-order solution and NCM.

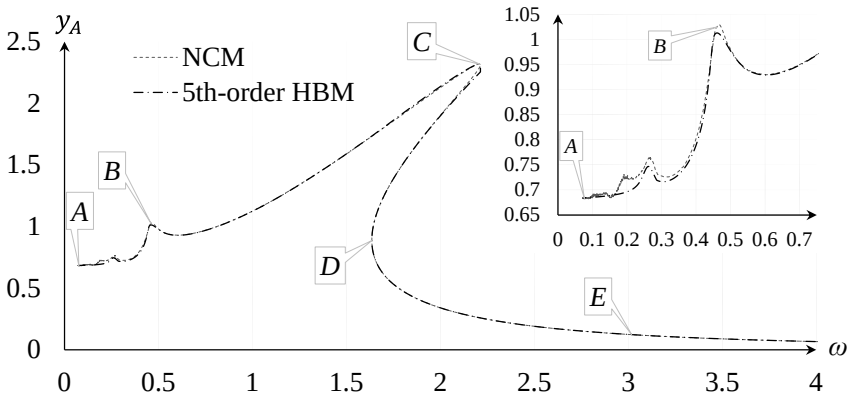


Figure 3. FRCs obtained by the 5th-order solution and NCM.

The 5th-order HBM formulation is employed to address residual inaccuracies in lower-order approximations. It is seen from Figure 3 that the 5th-order solution is better than the 3rd-order solution, particularly in the range of superharmonic resonances. As evidenced in Figure 3, this 5th-order solution reduces local errors 11% (3rd-order) to below 3% (5th-order) when compared with the NCM reference in the previously problematic second peak of *A*–*B* segment. For the first superharmonic peak at point *B*, the relative error decreases significantly with higher HBM orders, from 23% (1st-order) to 5% (3rd-order) and to under 2% (5th-order).

From the above analysis, a general trend is observed: the first-order solution captures the primary resonance peak, while the third-order solution not only improves the primary peak but also predicts the first superharmonic resonance peak. The fifth-order solution further extends this pattern by identifying the second superharmonic resonance peak and simultaneously enhancing the accuracy of both the primary and first superharmonic peaks. This behavior continues with higher-order solutions, where each additional order contributes new superharmonic peaks while refining all existing resonance predictions.

The appearance of superharmonic resonance peaks in higher-order HBM solutions can be attributed to the nonlinear coupling between harmonic components of the system response. In nonlinear systems, higher-order harmonics are generated due to the nonlinear restoring forces, which introduce spectral content at integer multiples of the excitation frequency. When these higher harmonics coincide with the system's natural frequencies, superharmonic resonances occur. This behavior is characteristic of nonlinear systems with stiffness or damping nonlinearities, where energy transfer between modes leads to additional peaks in the frequency response. Similar phenomena have been observed in [17,19,30], further validating the physical consistency of the observed results.

The relative error of the result obtained by HBM to that obtained by NCM is calculated by

$$relative\ error = \left| \frac{y_{A,\mathrm{NCM}} - y_{A,\mathrm{HBM}}}{y_{A,\mathrm{NCM}}} \right| \times 100\% \tag{17}$$

where $y_{A,HBM}$ and $y_{A,NCM}$ denote the amplitude obtained by HBM and NCM, respectively.

Relative errors for HBM solutions of different orders are shown in Figures 4, 5 and 6 for FRC's segments *A*–*C*, *C*–*D*, and *D*–*E*, respectively. Analysis of these results yields the following conclusions:

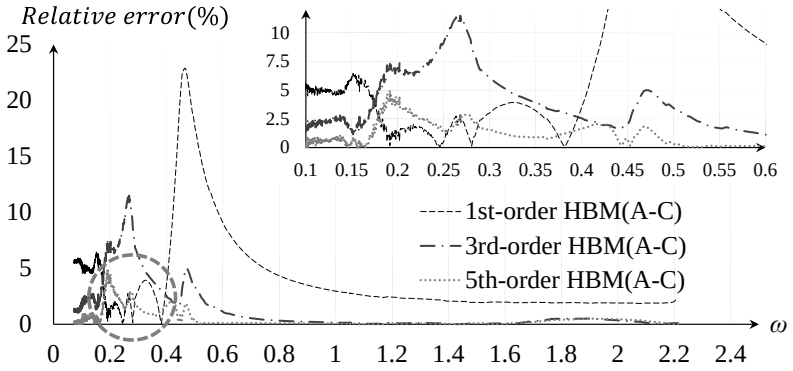


Figure 4. Relative errors in segment *A–C* (Example 1).

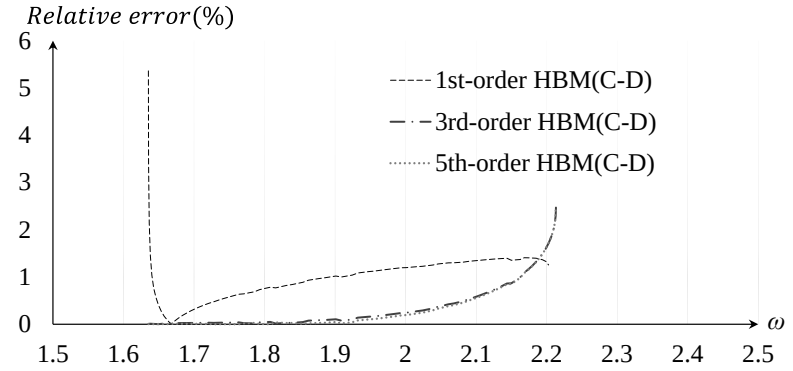


Figure 5. Relative errors in segment *C–D* (Example 1).

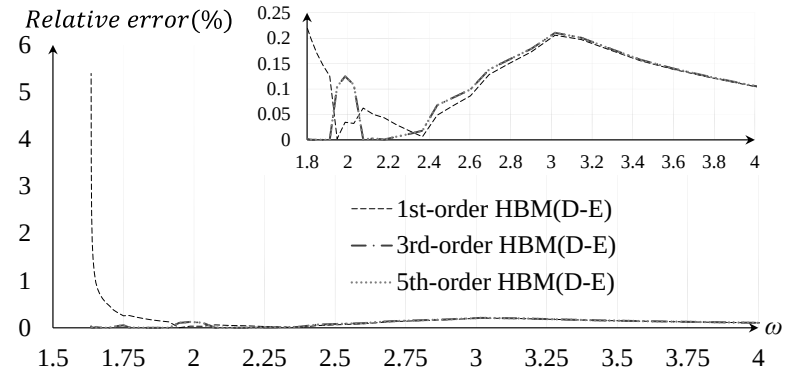


Figure 6. Relative errors in segment *D–E* (Example 1).

(1) For segment *A–C* in Figure 4, the higher-order solution demonstrates better agreement with NCM results compared to the lower-order solution, with the exception occurring when $\omega \in [0.176398, 0.393724]$ (indicated by a dashed circle). Within the dashed circle, the 5th-order solution exhibits better accuracy than the 1st-order one, except within four specific frequency ranges: $[0.178184, 0.178545]$, $[0.179639, 0.254389]$, $[0.267829, 0.286611]$, and $[0.375192, 0.388944]$. In addition, the 5th-order solution also provides more accurate results than the 3rd-order solution throughout segment *A–C*, except for the interval on the upper stable branch $[1.90077, 2.17547]$.

(2) Analysis of segments *C–D* and *D–E* reveals that the 3rd-order solution generally achieves better accuracy than the 1st-order solution, with exceptions of some local intervals $\omega \in [2.1897, 2.20277]$ (Figure 5) and $\omega \in [1.94744, 2.02949] \cup [2.36676, 4]$ (Figure 6). Notably, relative errors remain below

0.225% for all solution orders (1st to 5th) when $\omega \in [2.36676, 4]$. Although the 1st-order solution demonstrates local advantages in specific frequency intervals, these minor improvements become insignificant when compared to its substantially larger errors at the left ends (Figures 5 and 6).

(3) Comparative analysis of segments *C–D* and *D–E* indicates nearly identical performance between 3rd and 5th-order solutions (Figures 5 and 6), confirming that the 3rd-order solution delivers sufficient accuracy for both the unstable branch and lower stable branch.

(4) Figure 5 demonstrates that the first-order HBM solution exhibits significant errors for $\omega < 1.667$. A distinct minimum occurs at $\omega \approx 1.667$ due to zero-crossing of the relative error in this frequency region, corresponding to a temporary exact cancellation point before the error magnitude increases again for $\omega > 1.667$. This characteristic behavior is explained by error cancellation effects when the numerical error passes through zero within specific frequency ranges.

The error analysis reveals that higher-order solutions generally provide greater accuracy than lower-order solutions on the upper stable branch. However, specific observations indicate that at certain discrete points and within lower frequency intervals of this branch, the first-order solution may unexpectedly demonstrate smaller errors than its higher-order counterparts. For the unstable branch and lower stable branch, the third-order solution represents an optimal compromise, balancing solution accuracy with computational efficiency while avoiding excessive complexity.

4.2. Example 2: oscillator with nonlinear damping and restoring forces

Consider a nonlinear oscillator system characterized by both nonlinear damping and restoring forces, governed by the equation:

$$\ddot{y} + 2\xi\omega_0\dot{y} + \eta\dot{y}^3 + \omega_0^2 y + \varepsilon y^3 = A\sin\omega t \tag{18}$$

Consistent with standard HBM procedures for damped Duffing systems, the 1st-order harmonic balance approximation produces the characteristic equation governing the response amplitude y_A as a function of excitation frequency ω:

$$\left(\frac{2\xi\omega_0}{A} + \frac{3\eta\omega^2 y^2}{4A}\right)^2 \omega^2 y_A^2 + \left(\frac{3\varepsilon}{4}y_A^2 + \omega_0^2 - \omega^2\right)^2 \frac{y_A^2}{A^2} - 1 = 0 \tag{19}$$

Assigning the following parameter values to Equation (19) $\xi = 0.1$, $\omega_0 = 1$, $A = 1$, $\varepsilon = 1$ and $\eta = 0.1$, the governing equation becomes:

$$\ddot{y} + 0.2\dot{y} + 0.1\dot{y}^3 + y + y^3 = \sin\omega t \tag{20}$$

The FRCs obtained by the 1st, 3rd and 5th-order HBM are shown in Figures 7, 8 and 9, respectively.

Figures 7, 8 and 9 demonstrate that the 1st-order solution captures the primary resonance peak, while the 3rd-order solution additionally predicts the first superharmonic resonance peak while improving the primary peak accuracy, and the 5th-order solution further identifies the second superharmonic resonance peak while enhancing both the primary and first superharmonic peaks. This hierarchical improvement pattern, where higher-order solutions progressively capture additional superharmonic peaks while refining lower-order results, mirrors the behavior observed in damped Duffing oscillators.

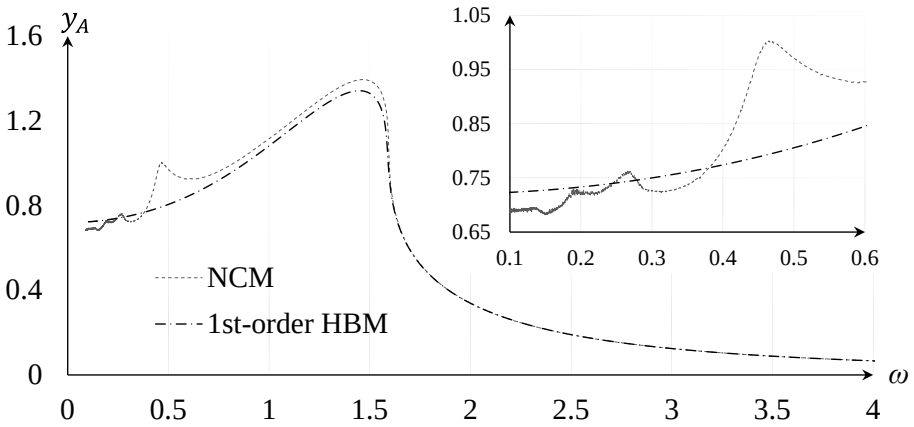


Figure 7. FRCs obtained by the 1st-order solution and NCM.

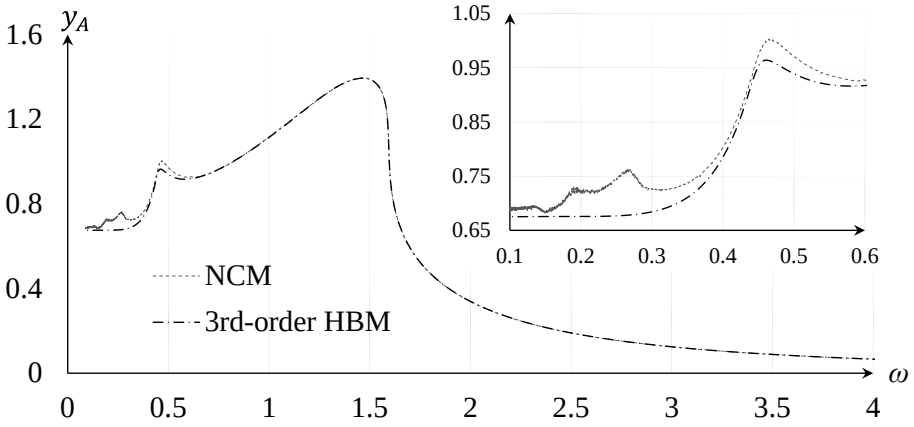


Figure 8. FRCs obtained by the 3rd-order solution and NCM.

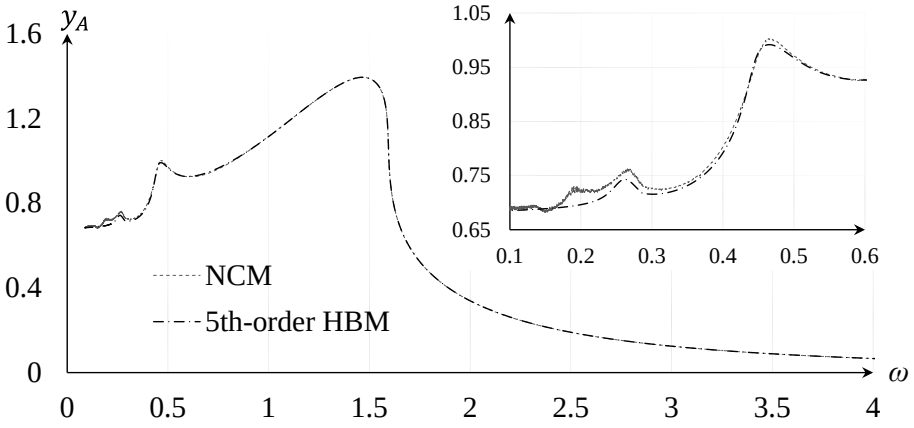


Figure 9. FRCs obtained by the 5th-order solution and NCM.

In this bifurcation-free case, Figure 10 provides a comprehensive comparison of relative errors across all solution orders. The 5th-order solution demonstrates superior accuracy overall, with relative errors below 5%, compared to 11% for the 3rd-order and 21% for the 1st-order solutions. However, localized exceptions exist where: (1) the 5th-order solution underperforms the 1st-order solution in

some local intervals [0.181652,0.258748], [0.262815,0.285243], [0.373519,0.38769], [3.7998,4.45955] and [2.01483,3.38675]; (2) the 5th-order solution is less accurate than the 3rd-order solution in [0.639549,0.890115], [1.21722,1.24825], [1.38646,1.39883], [1.49039,1.49186], [1.54792,1.57578], [1.59371,1.59857], [1.61903,1.62103] and [1.8536,1.87231]. This behavior primarily stems from error cancellation effects when the numerical error repeatedly crosses zero within specific frequency intervals. Due to the oscillatory nature of truncation errors, lower-order solutions may coincidentally align better with the true solution in certain frequency ranges, while higher-order approximations can introduce over-correction from their additional terms.

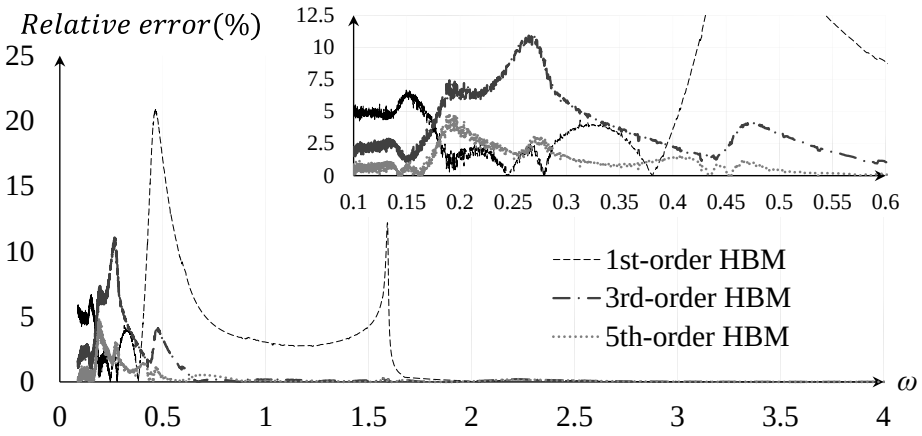


Figure 10. Relative errors of (Example 2).

The observed phenomenon where each two-order increase in HBM yields an additional SHR peak stems fundamentally from the odd-nonlinearity characteristics of the Duffing oscillator. In this system with only odd-order nonlinear terms, all even-harmonic coefficients in the HBM solution must vanish ($a_{2i} \equiv 0$ and $b_{2i} \equiv 0$) due to the system's symmetry properties. When non-zero coefficients exist for all harmonic components (which for odd systems occurs only at odd multiples of ω), each incremental HBM order captures an additional SHR peak. Therefore, the two-order increment phenomenon emerges due to the exclusively odd-ordered nonlinearity in the analyzed system. Specifically, while first-order HBM resolves only the fundamental harmonic (ω), third-order HBM captures the 3ω component (generating the first superharmonic resonance peak), and fifth-order HBM incorporates the 5ω component (producing the second superharmonic resonance peak).

5. Conclusions

This study investigates the responses of both a damped Duffing oscillator and an oscillator with cubic nonlinear damping and restoring forces using 1st-, 3rd-, and 5th-order harmonic balance methods (HBM). Particular attention is given to responses near superharmonic resonance frequencies. Numerical analysis reveals that for every two-order increasing in HBM, an additional peak appears in the SHR region of FRC for the system with exclusively odd-order nonlinearities, enhancing the accuracy of results:

(1) The 1st-order solution approximates the primary resonance peak, including its amplitude and frequency response. However, this approximation does not predict peaks at superharmonic resonance frequencies, as these require higher-order HBM for precise resolution.

(2) The 3rd-order solution captures both the first superharmonic resonance peak and improves the primary resonance peak accuracy;

(3) The 5th-order solution further identifies the second superharmonic resonance peak while enhancing the accuracy of both primary and first superharmonic peaks.

Although the higher-order solutions generally outperform the lower-order ones, they may not always yield higher solution accuracy in some local intervals near superharmonic resonance. This study reveals that the phenomenon of localized accuracy reduction occurs only in specific frequency intervals. Nevertheless, the overall trend of higher-order HBM solutions providing improved accuracy remains clearly demonstrated in both examples. It should be noted, however, that localized inaccuracies may still persist in some certain frequency ranges.

Acknowledgments

This paper's results were achieved with the support of S & T Program of Hebei (No. 24461901D) and The Research Committee of the University of Macau (Grant No. MYRG-GRG2024-00111-FST).

Author's contribution

Conceptualization, Guo-Peng Bai and Guo-Kang Er; methodology, Guo-Peng Bai and Guo-Kang Er; software, Guo-Peng Bai; data curation, Guo-Peng Bai; writing—original draft preparation, Guo-Peng Bai; writing—review and editing, Huanping Li, Guilin Wen and Guo-Kang Er; visualization, Huanping Li; supervision, Guilin Wen; project administration, Guilin Wen; funding acquisition, Guo-Peng Bai and Guo-Kang Er. All authors have read and agreed to the published version of the manuscript.

Conflicts of interests

The authors declare no conflict of interest.

References

[1] Caughey TK. Equivalent linearization techniques. *J. Acoust. Soc. Am.* 1963, 35(11):1706–1711.

[2] Nayfeh AH, Mook DT. *Nonlinear Oscillations*, 1st ed. Hoboken: John Wiley & Sons, 1995.

[3] Bhattacharjee JK, Mallik AK, Chakraborty S. An introduction to nonlinear oscillators: a pedagogical review. *Indian J. Phys.* 2007, 81(11):1115–1175.

[4] Chattopadhyay R, Chakraborty S. Equivalent linearization finds nonzero frequency corrections beyond first order. *Eur. Phys. J. B* 2017, 90(116):1–4.

[5] Peyton Jones JC, Yaser KSA. Recent advances and comparisons between harmonic balance and Volterra-based nonlinear frequency response analysis methods. *Nonlinear Dyn.* 2018, 91:131–145.

[6] Baily EM. Steady-state harmonic analysis of nonlinear networks. Doctoral Thesis, Stanford University, 1968.

[7] He J. Preliminary report on the energy balance for nonlinear oscillations. *Mech. Res. Commun.* 2002, 29(2–3):107–111.

[8] Guo Z, Leung AYT. The iterative homotopy harmonic balance method for conservative Helmholtz–Duffing oscillators. *Appl. Math. Comput.* 2010, 215(9):3163–3169.

[9] Nayfeh AH. *Perturbation methods*, 1st ed. Hoboken: John Wiley & Sons, 2000.

[10] Ahmad MZ, Hasan MK. A new fuzzy version of Euler's method for solving differential equations with fuzzy initial values. *Sains Malays.* 2011, 40(6):651–657.

[11] Fehlberg E. Classical fifth-, sixth-, seventh-, and eighth-order Runge-Kutta formulas with stepsize control. 1968. Available: https://ntrs.nasa.gov/citations/19680027281 (accessed on 19 September 2024).

[12] Nourazar S, Mirzabeigy A. Approximate solution for nonlinear Duffing oscillator with damping effect using the modified differential transform method. *Sci. Iran.* 2013, 20(2):364–368.

[13] Hackl J, Wacker H, Zulehner W. An efficient step size control for continuation methods. *BIT Numer. Math.* 1980, 20:475–485.

[14] Krauskopf B, Osinga HM, Galán-Vioque J. *Numerical Continuation Methods for Dynamical Systems*, 1st ed. Switzerland: Springer, 2007.

[15] Kim TC, Rook TE, Singh R. Super-and sub-harmonic response calculations for a torsional system with clearance nonlinearity using the harmonic balance method. *J. Sound Vib.* 2005, 281(3–5):965–993.

[16] Nakhla M, Vlach J. A piecewise harmonic balance technique for determination of periodic response of nonlinear systems. *IEEE Trans. Circuits Syst.* 1976, 23(2):85–91.

[17] Lai SK, Lim CW, Wu B, Wang C, Zeng Q, *et al.* Newton–harmonic balancing approach for accurate solutions to nonlinear cubic–quintic Duffing oscillators. *Appl. Math. Modell.* 2009, 33(2):852–866.

[18] Liu L, Kalmár-Nagy T. High-dimensional harmonic balance analysis for second-order delay-differential equations. *J. Vib. Control* 2010, 16(7–8):1189–1208.

[19] Luongo A, Zulli D. Aeroelastic instability analysis of NES-controlled systems via a mixed multiple scale/harmonic balance method. *J. Vib. Control* 2014, 20(13):1985–1998.

[20] Hosen MA, Chowdhury MSH. Solution of cubic-quintic Duffing oscillators using harmonic balance method. *Malays. J. Math. Sci.* 2016, 10:181–192.

[21] Niu J, Shen Y, Yang S, Li S. Higher-order approximate steady-state solutions for strongly nonlinear systems by the improved incremental harmonic balance method. *J. Vib. Control* 2018, 24(16):3744–3757.

[22] Taghipour J, Khodaparast HH, Friswell MI, Shaw AD, Jalali H, *et al.* Harmonic-balance-based parameter estimation of nonlinear structures in the presence of multi-harmonic response and force. *Mech. Syst. Signal Process.* 2022, 162:108057.

[23] Minorsky N. *Introduction to Non-linear Mechanics: Topological Methods, Analytical Methods, Non-linear Resonance, Relaxation Oscillations*, 1st ed. Michigan: Ann Arbor [Mich.]: J. W. Edwards, 1947.

[24] Yang J, Sanjuán MAF, Liu HG. Vibrational subharmonic and superharmonic resonances. *Commun. Nonlinear Sci. Numer. Simul.* 2016, 30(1–3):362–372.

[25] Uspensky B, Avramov K, Nikonov O. Nonlinear modes of piecewise linear systems forced vibrations close to superharmonic resonances. *Proc. Inst. Mech. Eng., Part C: J. Mech. Eng. Sci.* 2019, 233(23–24):7489–7497.

[26] Li Z, He Y, Lei J, Guo S, Liu D. Experimental and analytical study on the superharmonic resonance

of size-dependent cantilever microbeams. *J. Vib. Control* 2019, 25(21–22):2733–2748.

[27] Zhang X, Gao M, Hao Y. The 1/3rd subharmonic and 3rd superharmonic resonance of a shape memory alloy (SMA) laminated beam. *J. Theor. Appl. Mech.* 2021, 59(1):27–41.

[28] Chapra S, Canale R. *Numerical methods for engineers*, 7th ed. New York: Mcgraw-hill, 2010.

[29] Dhooge A, Govaerts W, Kuznetsov YA, Meijer HGE, Sautois B. New features of the software MatCont for bifurcation analysis of dynamical systems. *Math. Comput. Modell. Dyn. Syst.* 2008, 14(2):147–175.

[30] Du H, Er G, Lu V. Parameter-splitting perturbation method for the improved solutions to strongly nonlinear systems. *Nonlinear Dyn.* 2019, 96:1847–1863.